Fabrication of CuO/ZnO composite films with cathodic co-electrodeposition and their photocatalytic performance

Shouqiang Wei*, Yuye Chen, Yuyan Ma, Zhongcai Shao

School of Environmental and Chemical Engineering, Shenyang Ligong University, Nanping Middle Road 6 #, Shenyang 110159, Liaoning Province, PR China

ARTICLE INFO

ABSTRACT

CuO/ZnO composite films with different atomic Cu/Zn ratios were for the first time fabricated on indium tin oxide (ITO)-coated glass substrates via a cathodic co-electrodeposition route from baths containing $Zn(NO_3)_2$ and $Cu(CH_3COO)_2$. The obtained composite films were characterized with X-ray diffraction (XRD), scanning electron microscopy (SEM) and energy dispersive X-ray spectroscopy (EDS). Hexavalent chromium (Cr(VI)) was used as a model pollutant to evaluate their photocatalytic activity. For a bath containing $Zn(NO_3)_2$ with a certain concentration, the concentration of Cu^{2+} ions added into this bath play an important role in fabrication of CuO/ZnO composite films. When the Cu^{2+} concentration in a bath is lower, the obtained composite is a Cu-doped ZnO film. The electrodeposited CuO/ZnO composite films show higher photocatalytic activity towards reduction of Cr(VI) compared to pure ZnO both under UV and under UV–vis light illumination. Furthermore, the photocatalytic activity of CuO/ZnO composite films is related to their atomic Cu/Zn ratios. The mechanism of CuO/ZnO composite films for improvement in photocatalytic activity was also discussed.

© 2010 Elsevier B.V. All rights reserved.

1. Introduction

Photocatalytic treatment of organic or inorganic pollutants from water and air using semiconductors as photocatalysts has been a promising process among advanced oxidation technologies [1,2]. Semiconductor ZnO with broad-band-gap (3.2 eV) has been extensively investigated as semiconductor photocatalysts for the contaminant remediation [3–5]. However, ZnO can only absorb a small portion of solar spectrum in the UV region, which means that they does not allow the efficient utilization of visible light. Compared with those broad-band-gap semiconductors, the photoresponse of semiconductors with narrow-band-gap extends much more into the visible wavelength range. Nevertheless, the narrow-band-gap semiconductors exhibit low photocatalytic efficiency due to fast recombination rate for electron–hole pairs photogenerated on the semiconductors [6]. The reports in the literature indicated that coupling of a narrow-band-gap semiconductor with another having broad-band-gap results in a more efficient separation and consequently, a higher visible light induced photocatalytic activity compared with the single narrow-band-gap semiconductor [7]. In the past several years, composite semiconductors of ZnO coupled with narrow-band-gap semiconductor, including Fe_2O_3, WO_3, CdS, Cu_2O and CuO, have been reported

[8–11]. It is worth noting that most of CuO/ZnO composite are used for methanol synthesis, hydrogen production and gas sensor. More recently, CuO/ZnO nano-composites were prepared via coordination oxidation homogeneous co-precipitation method and used for photocatalytic degradation of methyl orange [12].

Electrodeposition has been received more attention as a method for the synthesis of oxide thin films due to its interesting characteristics for large area, low cost, generally low temperature and easily controlling of the film thickness [13]. A great number of unary oxides such as TiO_2, ZnO, WO_3 and Cu_2O have been prepared with electrodeposition [6,13–17]. On the other hand, very little information is available on the cathodic co-electrodeposition of multinary oxides. Pauporte et al. reported co-precipitation of zinc and europium oxides and co-precipitation of TiO_2 and WO_3 with cathodic electrodeposition [18].

Hexavalent chromium (Cr(VI)) is a carcinogenic contaminant in waste waters arising from industrial processes such as electroplating, leather tanning, or paint manufacture. The preferred treatment is reduction of Cr(VI) to the less harmful Cr(III), which can be precipitated in neutral or alkaline solutions as $Cr(OH)_3$. Compared with conventional reduction processes, photocatalytic reduction of Cr(VI) over semiconducting materials has some obvious advantages, such as no addition of other chemicals, operation at mild conditions and low cost [19]. The utilization of photocatalysis in reducing Cr(VI) has been reported in the literature since 1979 [20]. TiO_2, ZnO, WO_3, CdS and so on were used as photocatalysts for reduction of Cr(VI) under UV or visible light irradiation [21–24]. To

* Corresponding author. Tel.: +86 24 24681936; fax: +86 24 86259041.
E-mail address: weisq1961@126.com (S. Wei).

the best of our knowledge, there is no report on the photocataytic reduction of Cr(VI) over CuO/ZnO composite films.

In the present work, ZnO/CuO composite films have been successfully prepared with cathodic electrodeposition on indium tin oxide (ITO)-coated glass substrates from $Zn(NO_3)_2 + Cu(CH_3COO)_2$ aqueous solutions. The obtained composite films were characterized with X-ray diffraction (XRD), scanning electron microscopy (SEM) and energy dispersive X-ray spectroscopy (EDS). Hexavalent chromium (Cr(VI)) was used as a model pollutant to evaluate the photocatalytic activity of the ZnO/CuO composite films both under UV and UV–vis light irradiation.

2. Experimental

2.1. Materials

All chemicals were of analytic reagent grade and used as received. Except Potassium dichromate (from Tianjin Damao Chemical Reagent Factory, China), the other reagents were purchased from Sinopharm Chemical Reagent Co. Ltd., China. All solutions were prepared with distilled water. Cr(VI) stock solution (0.02 mol/L) was prepared by dissolving $K_2Cr_2O_7$ into distilled water.

2.2. Preparation of films

Before use, an indium tin oxide (ITO)-coated glass slide (2 cm × 5 cm) was rinsed successively in acetone, absolute ethanol and distilled water. Following the pre-treatment, the substrate was immediately transferred to a bath containing 0.5 mol/L $Zn(NO_3)_2$, in which the concentration of $Cu(CH_3COO)_2$ was 0 mmol/L, 1 mmol/L, 15 mmol/L and 30 mmol/L, respectively, and pH was in the range 4–6. Cathodic electrodeposition of CuO/ZnO composite films onto ITO substrates (each sample efficient area: 2 cm × 2.5 cm) was performed from the above baths at constant current density of 3 mA cm^{-2} for 15 min in an ordinary cell with a zinc plate used as the counter electrode. The deposition bath temperature was fixed at 65 °C.

2.3. Characterization of films

The morphology and elemental composition of the resulting films were examined with a scanning electron microscope equipped with an EDS facility (S3400, HITACHI, Japan). The crystalline structure of films was determined with an X-ray diffractometer (D/Max-RB, RIGAKU, Japan).

2.4. Photocatalytic reactions

The obtained films (efficient area: 5 cm^2) were placed inside 15 mL of Cr(VI) aqueous solutions (containing 0.2 mmol/L Cr(VI) and 0.4 mmol/L citric acid (CA), pH = 4.6) filled in a cylinder quartz tube. A 20 W high-pressure mercury lamp with a maximum emission at 365 nm and a 300 W metal halide lamp (λ > 365 nm) were used as UV and UV–vis light sources, and the illumination density available at the film surface is about 2 mW/cm^2 and 14 mW/cm^2, respectively. The concentrations of Cr(VI) during the photocatalytic reactions were determined spectrophotometrically by measuring the absorbance at 349 nm with a spectrophotometer (721E, Shanghai Spectra Instrument Co. Ltd., China). Photocatalytic activity of the CuO/ZnO composite films was evaluated with Cr(VI) residual % which can be expressed as follows:
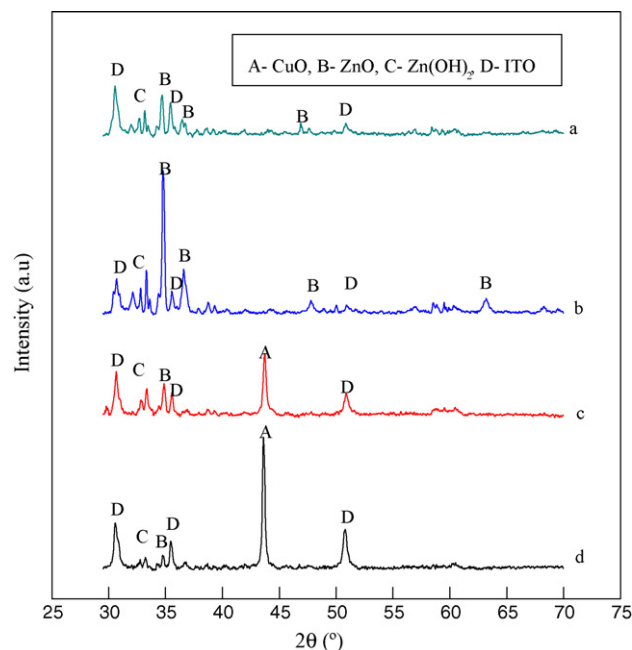
$$Cr(VI) \text{ residual } \% = \frac{C_t}{C_0}\% \tag{1}$$

Fig. 1. XRD patterns of the composite films obtained from electrodeposition baths containing 0.5 mol/L $Zn(NO_3)_2$ and different Cu^{2+} concentrations: 0 mmol/L (a), 1 mmol/L (b), 15 mmol/L (c) and 30 mmol/L (d), respectively.

where C_0 and C_t are the concentrations of Cr(VI) before and after photocatalytic reactions. All the photocatalytic experiments were carried out without stirring.

3. Results and discussion

3.1. Characterization of films

Fig. 1 shows XRD patterns of the films prepared with different concentrations of Cu^{2+} (0 mmol/L, 1 mmol/L, 15 mmol/L, and 30 mmol/L). The peaks indicated by "D" come from the ITO substrates. The peaks marked with "B" correspond to ZnO (JCPDS, 36-1451), indicating that ZnO has been deposited on ITO-coated glass substrates at each concentration of Cu^{2+}. When Cu^{2+} concentrations in electrodeposition baths are 15 mmol/L and 30 mmol/L, respectively, the diffraction peaks (marked with "A") matching with CuO (JCPDS, 49-1830) were observed, which clearly indicates that co-precipitation of CuO and ZnO takes place and CuO/ZnO composite films have been successfully fabricated on ITO-coated glass substrates. The peaks marked with "C" come from $Zn(OH)_2$, which may mean that the dehydration of $Zn(OH)_2$ into ZnO is incomplete in our experiments.

In the previous work [25], It was found that the copper oxide potentiostatically electrodeposited from an acetate bath is cuprous oxide (Cu$_2$O) rather than cupric oxide (CuO). And the following formation mechanism for cuprous oxide from acetate bath has been proposed.

$$2Cu^{2+} + H_2O + 2e^- \rightarrow Cu_2O + 2H^+ \tag{2}$$

However, in the case of present baths containing $Zn(NO_3)_2$ and $Cu(CH_3COO)_2$, because the nitrate system has a more positive redox potential (E^0 = 0.93 V vs. SHE, pH = 0) than that of Cu(II)/Cu(I) redox couple (E^0 = 0.16 V vs. SHE, pH = 0) [26] and furthermore, the concentration of NO_3^- is much higher than that of Cu^{2+}, the reduction of NO_3^- at the surface of electrode occurs predominantly according to Eq. (3)

$$NO_3^- + H_2O + 2e^- \rightarrow NO_2^- + 2OH^- \tag{3}$$

This reduction reaction leads to a pH increase in the vicinity of the electrode and a local supersaturation due to the release of hydroxide ions. In the present baths, apart from the reaction of these hydroxide ions with zinc ions to form ZnO on the electrode surface (Eq. (4)) [27]

$$Zn^{2+} + 2OH^- \rightarrow Zn(OH)_2 \rightarrow ZnO + H_2O \qquad (4)$$
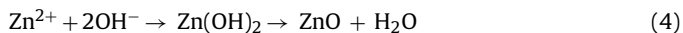
a precipitation reaction for CuO similar to that for ZnO may simultaneously take place on the same electrode surface (Eq. (5)). This process is the so-called cathodic co-electrodeposition [18].
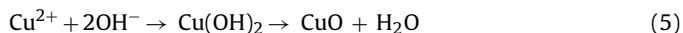
$$Cu^{2+} + 2OH^- \rightarrow Cu(OH)_2 \rightarrow CuO + H_2O \qquad (5)$$

Fig. 2 shows the EDS distribution of elements for the composite films prepared with different Cu^{2+} concentrations in the baths (1 mmol/L, 15 mmol/L and 30 mmol/L). The atomic Cu/Zn ratios in the composite films were calculated from the data to be 0.02, 0.73 and 1.10 corresponding to those Cu^{2+} concentrations, respectively. It is indicated that the atomic Cu/Zn ratio in a composite film can be tuned over a large composition range just by varying the molar ion ratio in the deposition bath. For the composite film (atomic Cu/Zn ratio: 0.02) obtained from a bath containing 1 mmol/L Cu^{2+}, no diffraction peaks corresponding to CuO were observed (see Fig. 1), which means that the co-deposition process for CuO and ZnO do not occur. The reason may be attributed to the fact that the local supersaturation is not achieved for CuO due to lower Cu^{2+} concentration. Considering that Cu^{2+} (0.072 nm) and Zn^{2+} ions (0.074 nm) have almost the same ionic radius [28], Cu^{2+} ions may be incorporated into ZnO lattice in such a case. As a result, Cu-doped ZnO films may be obtained.

It is worth noting that the atomic Cu/Zn ratio in a CuO/ZnO composite film is much higher than that in a corresponding deposition bath (0.03 and 0.06 corresponding to 15 mmol/L and 30 mmol/L of Cu^{2+} concentrations, respectively). This phenomenon can be attributed to the difference of solubility between $Cu(OH)_2$ and $Zn(OH)_2$. Solubility constants (pKs) for $Cu(OH)_2$ and $Zn(OH)_2$ at room temperature are 18.59 and 16.92, respectively [29].

SEM micrographs of pure ZnO and composite films are shown in Fig. 3. No significant morphological differences between pure ZnO (corresponding to atomic Cu/Zn ratio being 0) and the composite
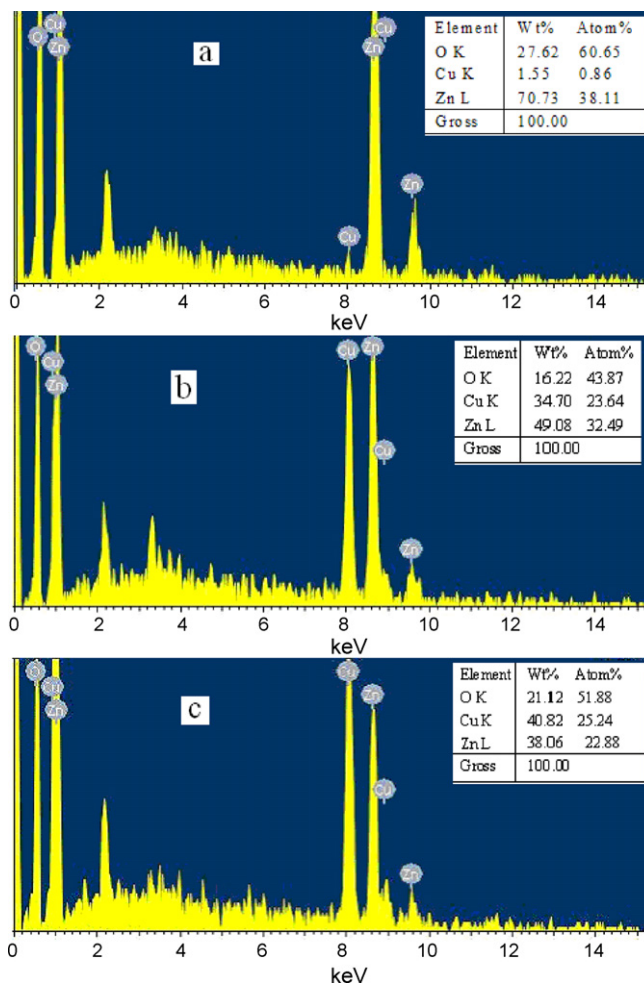

Element	Wt%	Atom%
O K	27.62	60.65
Cu K	1.55	0.86
Zn L	70.73	38.11
Gross	100.00	

Element	Wt%	Atom%
O K	16.22	43.87
Cu K	34.70	23.64
Zn L	49.08	32.49
Gross	100.00	

Element	Wt%	Atom%
O K	21.12	51.88
Cu K	40.82	25.24
Zn L	38.06	22.88
Gross	100.00	

Fig. 2. EDS element distribution of the composite films obtained from electrodeposition baths containing 0.5 mol/L $Zn(NO_3)_2$ and different Cu^{2+} concentrations: 1 mmol/L (a); 15 mmol/L (b) and 30 mmol/L (c), respectively.
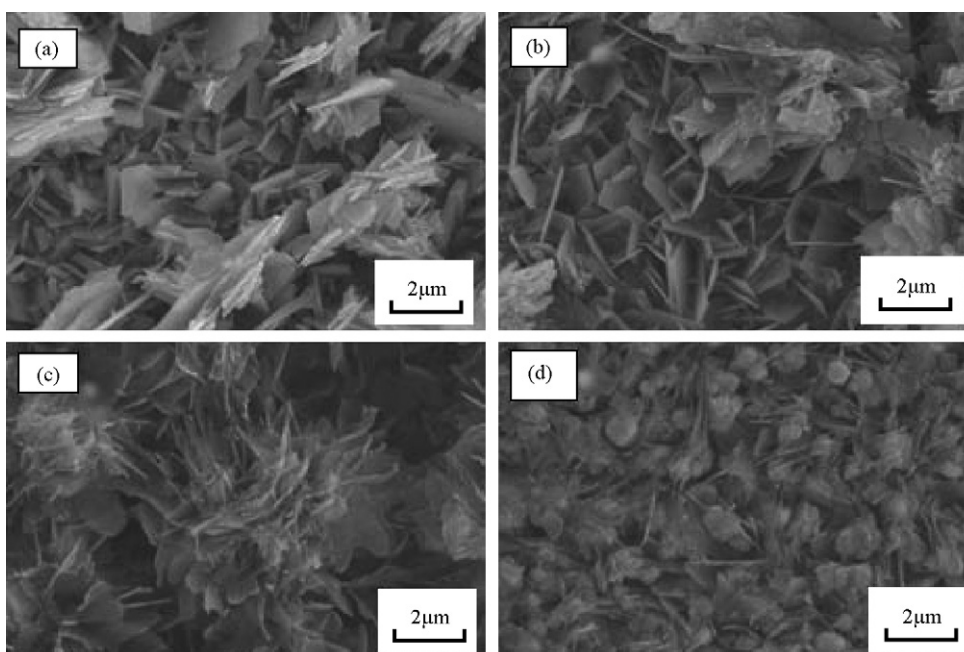

Fig. 3. SEM micrographs of the composite films with different atomic Cu/Zn ratios: 0 (a), 0.02 (b), 0.73 (c) and 1.10 (d), respectively.
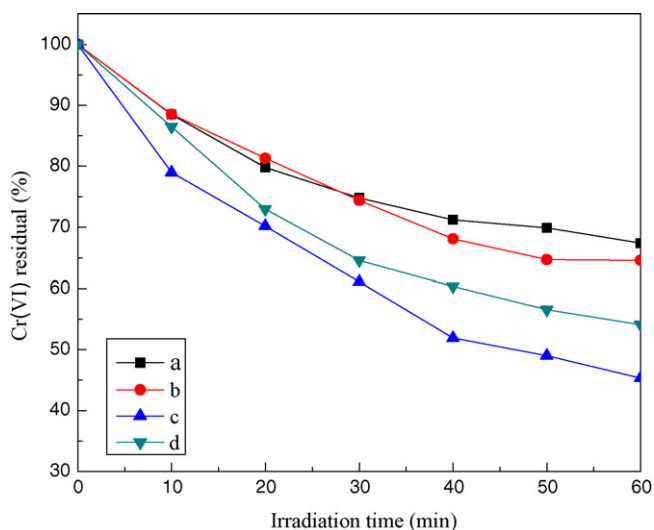
Fig. 4. Photocatalytic reduction of Cr(VI) under UV light illumination over the composite films with different atomic Cu/Zn ratios: 0 (a), 0.02 (b), 0.73 (c) and 1.10 (d), respectively.

film with the atomic Cu/Zn ratio being 0.02 (i.e., the Cu-doped ZnO film) can be noticed. Compared with pure ZnO, the morphologies of CuO/ZnO composite films are changed significantly. Furthermore, the atomic Cu/Zn ratios have great influence on the morphologies of the composite films. When Cu/Zn ratio is 0.73, flower-like superstructures are obtained. As Cu/Zn ratio increases to 1.10, the morphologies of the composite films evolve to assemblies of flakes and grains.

3.2. Photocatalytic activity

Initially, direct photolysis of Cr(VI) in the absence of catalysts and adsorption of Cr(VI) onto catalysts under dark conditions without light illumination were performed, respectively. The negligible change in Cr(VI) concentrations was observed for each experiment. These results indicate that the reduction of Cr(VI) is caused by photocatalytic reaction on catalysts under light illumination.

The photocatalytic reduction of Cr(VI) was carried out under UV and UV–vis light illumination over the composite films with different atomic Cu/Zn ratios, respectively. The change in Cr(VI) concentrations with illumination time is depicted in Figs. 4 and 5.
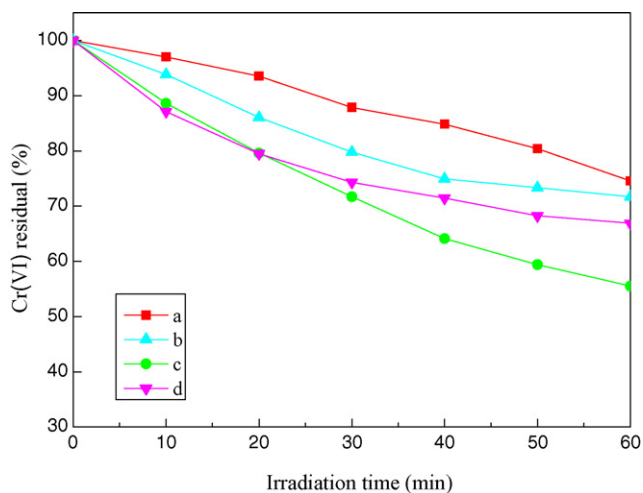
For comparison, the results obtained from pure ZnO is included in the same figures. It can be seen that the Cr(VI) residual (%) at given time during the photocatalytic reduction period over the composite films is lower that over pure ZnO both under UV and under UV–vis light illumination. The results indicate that the composite films are photocatalytically more active than the corresponding pure ZnO. Moreover, the CuO/ZnO composite film exhibits a higher photocatalytic activity than that Cu-doped ZnO film. It should be noted that the CuO/ZnO composite film (atomic Cu/Zn ratio: 1.10) is less active than that (atomic Cu/Zn ratio: 0.73). The improvement in photocatalytic activity of the composite films can be explained as follows:

Under UV light illumination, Cu-doped ZnO films show a slightly higher photocatalytic activity than that of pure ZnO films (see Fig. 4). This result indicates that Cu(II) plays a minor role in UV light-driven photocatalytic reduction of Cr(VI) over Cu-doped ZnO. However, the photocatalytic activity of Cu-doped ZnO films is enhanced obviously compared with pure ZnO films under UV–vis light illumination. The photocatalytic activity enhancement of ZnO when doped with small quantities of Cu(II) under UV–vis light illumination may be resulted from the formation of Cu(I) induced by visible light. As shown in Fig. 6, ZnO cannot be activated by visible light due to its broad-band-gap, but electrons in the valence band (VB) of ZnO can be directly transferred to Cu(II) and consequently, holes in the VB of ZnO and Cu(I) are formed [30]. The holes produced in the VB of ZnO oxidize CA, and meanwhile the formed Cu(I) reduces Cr(VI) to Cr(III) and itself will return to original Cu(II) form.

As a result, the photocatalytic activity of Cu-doped ZnO films is improved. On the other hand, as atomic Cu/Zn ratio is increased to 0.73 or 1.10, the enhancement of activity for CuO/ZnO composite films should be mainly explained in terms of efficient separation of charges photogenerated in CuO/ZnO heterostructures in addition to the above-mentioned electron transfer.

CuO is a p-type semiconductor with narrow-band-gap (ca. 1.7 eV) [31], and it may have acted as a visible light-driven photocatalyst; however, it was found that CuO shows very low photocatalytic activity [32], which may be attributed to the inefficient charge transport within CuO [6]. The enhanced activity for CuO/ZnO both under UV and UV–vis light irradiation can be interpreted using a schematic diagram of the energy band structure of CuO/ZnO heterojunction shown in Fig. 7.
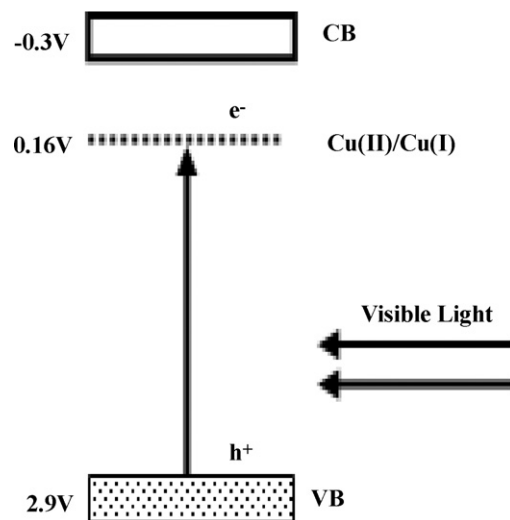

Fig. 5. Photocatalytic reduction of Cr(VI) under UV–vis light illumination over the composite films with different atomic Cu/Zn ratios: 0 (a), 0.02 (b), 0.73 (c) and 1.10 (d), respectively.

Fig. 6. Energy diagram of ZnO and redox potential of Cu(II)/Cu(I) (energy levels are referred to NHE).
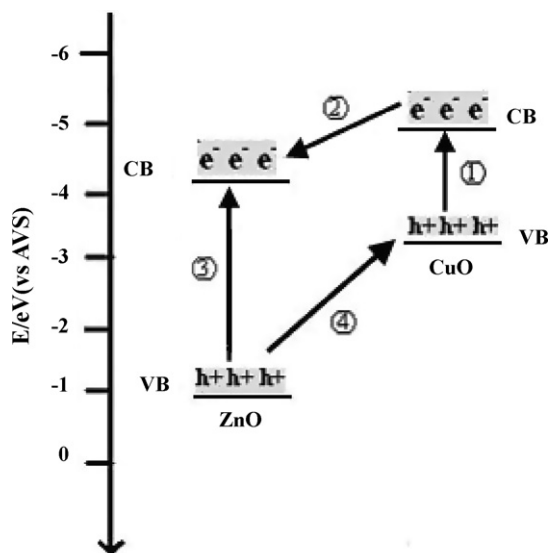
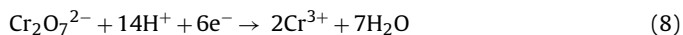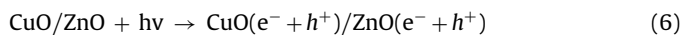**Fig. 7.** Energy band diagram for ZnO/CuO heterostructure materials in contact, showing corresponding valence and conduction band positions and photogenerated hole and electron transfer.

Under UV light illumination, both CuO and ZnO can be excited according to process (1) and (3), respectively. The conduction band (CB) edge of CuO (-4.96 eV vs. absolute vacuum scale (AVS)) is higher than that of ZnO (-4.19 eV vs. AVS); the valence band (VB) edges of CuO and ZnO are situated at -3.26 eV and -0.99 eV vs AVS, respectively [33]. From thermodynamic view points, the photogenerated electrons transfer from CB of CuO to that of ZnO, while the photogenerated holes immigrate in the opposite direction from VB of ZnO to that of CuO. Consequently, more electrons are accumulated in CB of ZnO and consumed for reduction of Cr(VI). Thus CuO/ZnO composite films show higher photocatalytic activity than that of pure ZnO films. The photocatalytic reduction process for Cr(VI) over CuO/ZnO composite films under UV light illumination can be proposed as follows:

$$CuO/ZnO + h\nu \rightarrow CuO(e^- + h^+)/ZnO(e^- + h^+) \tag{6}$$

$$CuO(e^- + h^+)/ZnO(e^- + h^+) \rightarrow CuO(h^+)/ZnO(e^-) \tag{7}$$

$$Cr_2O_7^{2-} + 14H^+ + 6e^- \rightarrow 2Cr^{3+} + 7H_2O \tag{8}$$

$$h^+ + CA \rightarrow oxidation\ products \tag{9}$$

In the case of UV–vis light illumination, ZnO can only be excited by a small portion of UV light from the UV–vis light source, so it shows lower photocatalytic activity compared to UV light illumination (see Figs. 4 and 5). Under visible light illumination, the interband transition of electrons within CuO (process (1)) still occurs, while ZnO cannot be activated due to its broad-band-gap, i.e., process (3) does not take place. In such a case, the mechanism for photogenerated charges transfer between the two semiconductor materials is different from that under UV light illumination, which can be expressed as follows:

$$CuO/ZnO + h\nu \rightarrow CuO(e^- + h^+)/ZnO \tag{10}$$

$$CuO(e^- + h^+)/ZnO \rightarrow CuO(h^+)/ZnO(e^-) \tag{11}$$
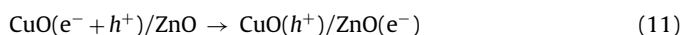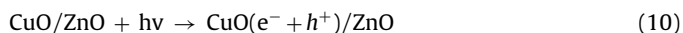
Based on the above-mentioned reason, it is deduced that CuO/ZnO composite films also exhibit higher photocatalytic activity for reduction of Cr(VI) in comparison with pure ZnO films even under visible light irradiation. The exact reason why CuO/ZnO composite film (atomic Cu/Zn ratio: 1.10) is less active than that (atomic Cu/Zn ratio: 0.73) is not clear, but there are several possible explanations. For example, the morphologies of the latter differ

remarkably from the former (see Fig. 3), which may indicate that the interfaces between CuO and ZnO are also changed significantly. It was found that the interfaces among the particles of a semiconductor composite play an important role in the photocatalytic reaction [34]. The details of the mechanism for the effect of atomic Cu/Zn ratio on the photocatalytic activity of CuO/ZnO composite films are under investigation.

4. Conclusions

CuO/ZnO composite films have been successfully fabricated on ITO-coated glass substrates via a cathodic co-electrodeposition route from baths containing Zn(NO$_3$)$_2$ and Cu(CH$_3$COO)$_2$. For a bath containing Zn(NO$_3$)$_2$ with a certain concentration, the concentration of Cu^{2+} ions added into this bath play an important role in cathodic co-electrodeposition of CuO/ZnO composite films. When the Cu^{2+} concentration in a bath is lower, the obtained composite is Cu-doped ZnO film. The atomic Cu/Zn ratio in the obtained composite films can be tuned over a large composition range just by varying the molar ion ratio in the deposition baths. And the atomic Cu/Zn ratio in a composite film is much higher than that in a corresponding deposition bath. CuO/ZnO composite films show higher photocatalytic activity towards reduction of Cr(VI) compared to pure ZnO both under UV and under UV–vis light illumination. The photocatalytic activity of CuO/ZnO composite films is related to their atomic Cu/Zn ratios. The enhanced activity of CuO/ZnO composite films may be mainly attributed to the efficient separation of charges photogenerated in CuO/ZnO heterostructures.

References

[1] A. Fujishima, T.N. Rao, D.A. Tryk, J. Photochem. Photobiol. C 1 (2000) 1.
[2] J. Yu, L. Qi, J. Hazard. Mater. 169 (2009) 221.
[3] S. Sakthivel, B. Neppolian, M.V. Shankar, B. Arabindoo, M. Palanichamy, V. Murugesan, Sol. Energy Mater. Sol. Cells 77 (2003) 65.
[4] E. Evgenidou, K. Fytianos, I. Poulios, Appl. Catal. B 59 (2005) 81.
[5] A. Shafaei, M. Nikazar, M. Arami, Desalination 252 (2010) 8.
[6] C.C. Hu, J.N. Nian, H. Teng, Sol. Energy Mater. Sol. Cells 92 (2008) 1071.
[7] J. Georgieva, S. Armyanov, E. Valova, I. Poulios, S. Sotiropoulos, Electrochem. Commun. 9 (2007) 365.
[8] S. Sakthivel, S.U. Geissen, D.W. Bahnemann, V. Murugesan, A. Vogelpohl, J. Photochem. Photobiol. A 148 (2002) 283.
[9] C. Xu, L. Cao, G. Su, W. Liu, H. Liu, Y. Yu, X. Qu, J. Hazard. Mater. 176 (2010) 807.
[10] I. Eswaramoorthi, V. Sundaramurthy, A.K. Dalai, Appl. Catal. A 313 (2006) 22.
[11] H.C. Yang, F.W. Chang, L.S. Roselin, J. Mol. Catal. A 276 (2007) 184.
[12] Z.L. Liu, J.C. Deng, J.J. Deng, F.F. Li, Mater. Sci. Eng. B 150 (2008) 99.
[13] Th. Pauporté, D. Lincot, Sol. Energy Mater. Sol. Cells 45 (2000) 3345.
[14] I. Zhitomirsky, L. Gal-Or, A. Kohn, H.W. Hennicke, J. Mater. Sci. 30 (1995) 5307.
[15] I. Shiyanovskaya, M. Hepel, J. Electrochem. Soc. 146 (1999) 243.
[16] J. Georgieva, S. Armyanov, E. Valova, Ts. Tsacheva, I. Poulios, S. Sotiropoulos, J. Electroanal. Chem. 585 (2005) 35.
[17] J. Georgieva, S. Armyanov, E. Valova, I. Poulios, S. Sotiropoulos, Electrochim. Acta 51 (2006) 2076.
[18] Th. Pauporté, A. Goux, A. Kahn-Harari, N. de Tacconi, C.R. Chenthamarakshan, K. Rajeshwar, D. Lincot, J. Phys. Chem. Solids 64 (2003) 1737.
[19] B. Xie, H. Zhang, P. Cai, R. Qiu, Y. Xiong, Chemosphere 63 (2006) 956.
[20] H. Yoneyama, Y. Yamashlta, H. Tamura, Nature 282 (1979) 817.
[21] X. Xu, H. Li, J. Gu, Chemosphere 63 (2006) 254.
[22] S. Chakrabarti, B. Chaudhuri, S. Bhattacharjee, A.K. Ray, B.K. Dutta, Chem. Eng. J. 153 (2009) 86.
[23] A. Watcharenwong, W. Chanmanee, N.R. de Tacconi, C.R. Chenthamarakshan, P. Kajitvichyanukul, K. Rajeshwar, J. Electroanal. Chem. 612 (2008) 112.
[24] S. Wang, Z. Wang, Q. Zhuang, Appl. Catal. B l (1992) 257.
[25] R.P. Wijesundera, M. Hidaka, K. Koga, M. Sakai, W. Siripala, Thin Solid Films 500 (2006) 241.
[26] A.J. Bard, R. Parsons, J. Jordan (Eds.), Standard Potentials in Aqueous Solution, Marcel Dekker, New York, 1985.
[27] T. Yoshida, D. Komatsu, N. Shimokawa, H. Minoura, Thin Solid Films 451–452 (2004) 166.
[28] C. Yu, X. Zhang, J. Xu, D. Yu, J. Chin. Electr. Microsc. Soc. 27 (2008) 2.
[29] J.A. Dean, Lange's Handbook of Chemistry, 15th ed., McGraw-Hill, 1999.
[30] H. Irie, S. Miura, K. Kamiya, K. Hashimoto, Chem. Phys. Lett. 457 (2008) 202.
[31] M.A. Butler, D.S. Ginley, J. Electrochem. Soc. 125 (1978) 228.
[32] T. Arai, M. Yanagida, Y. Konishi, Y. Iwasaki, H. Sugihara, K. Sayama, Catal. Commun. 9 (2008) 1254.
[33] Y. Xu, M.A.A. Schoonen, Am. Miner. 85 (2000) 543.
[34] Z. Liu, Z. Zhao, M. Miyauchi, J. Phys. Chem. C 113 (2009) 17132.